Functional α7 Nicotinic ACh Receptors on Astrocytes in Rat Hippocampal CA1 Slices

Jian-xin Shen and **Jerrel L. Yakel**

Laboratory of Neurobiology, National Institute of Environmental Health Sciences, National Institutes of Health, Department of Health and Human Services, P.O. Box 12233, 111 T.W. Alexander Drive, Research Triangle Park, NC 27709, USA yakel@niehs.nih.gov

Abstract

Although much is known about the functional expression of the neuronal nicotinic acetylcholine receptors (nAChRs) in various neuronal populations in the brain and elsewhere, much less is known about their expression and functional relevance in glial cells. The expression of functional nAChRs has been reported for cultured astrocytes; however, previous work has failed to detect nAChR-mediated responses in astrocytes in acute slices. In the current study, functional α7 nAChRs on astrocytes in the CA1 region of the rat hippocampus were studied in situ using whole-cell patch-clamp recording and two-photon calcium imaging techniques in acute slices. We found that astrocytes and the chondroitin sulfate proteoglycan NG2-expressing (i.e., NG2) cells did express functional α7 nAChRs. Although the amplitudes of the responses were small, they could be enhanced by the α7-selective positive allosteric modulator PNU-120596. Under these conditions, we found that in comparing the properties of these responses between astrocytes, NG2, and interneurons, there were differences in the kinetics and increases in intracellular calcium levels. This is the first demonstration of functional α7 nAChR-mediated current responses in astrocytes in acute hippocampal slices, data which may shed light on the role of α7 nAChRs in neuroprotection.

Keywords

Nicotinic receptor; Calcium signaling; Patch-clamp

Introduction

The neuronal nicotinic acetylcholine receptors (nAChRs) are cys-loop receptor/ligand-gated ion channels with wide distribution throughout the central and peripheral nervous system, where they are involved in a wide variety of important physiological functions, including cognitive functions such as learning and memory (Jones et al. 1999; Giniatullin et al. 2005; Levin et al. 2006; Dani and Bertrand 2007; Gay and Yakel 2007; Yakel 2010). Although much is known about their functional expression in various neuronal populations in the brain

and elsewhere, much less is known about their expression and functional relevance in non-neuronal cells. Of the major types of glial cells in the mammalian brain, including astrocytes, microglia, oligodendrocytes, and the chondroitin sulfate proteoglycan NG2-expressing (i.e., NG2) cells, the astrocytes are the predominant type (Agulhon et al. 2008). Glial cells not only express a variety of neurotransmitter receptors and ion channels, but also participate in synaptic signaling and plasticity in the brain (Araque et al. 2002; Agulhon et al. 2008; Fiacco et al. 2009).

The cognitive deficits associated with Alzheimer's disease (AD) may in part be caused by dysfunction in the α7 subtype of the neuronal nAChRs in the hippocampus (Jonnala and Buccafusco 2001; Kihara et al. 2001; Dineley 2007; Parri et al. 2011). However, conflicting reports have recently appeared as to whether knocking out the α7 nAChR subunit in an AD mouse model decreases (Dziewczapolski et al. 2009) or enhances (Hernandez et al. 2010) cognitive deficits associated with AD. In astrocytes, the α7 nAChRs are upregulated in AD (Teaktong et al. 2003; Xiu et al. 2005), and α7 nAChR-positive astrocytes are associated with the β-amyloid peptide (Aβ) and neuritic plaques in the AD brain (Nagele et al. 2003; 2004; Xiu et al. 2005; Yu et al. 2005). There is also an evidence for a role of α7 nAChRs in neuroprotection (Dineley 2007; Shen et al. 2009; Parri et al. 2011). For example, the protective effect of nicotine or 17β-estradiol against Aβ has been found to involve the α7 nAChR (Kihara et al. 1997; Svensson and Nordberg 1999; Jonnala and Buccafusco 2001). Therefore, astrocytes may be playing a role in AD and/or neuroprotection that depend in part on the function of the α7 nAChRs.

Although the expression of functional nAChRs has previously been reported for cultured astrocytes and microglia (Sharma and Vijayaraghavan 2001; Shytle et al. 2004), previous work has failed to detect nAChR-mediated responses in astrocytes in acute slices (Araque et al. 2002). Recently, Vélez-Fort et al. (2009) found that NG2 cells in acute hippocampal mouse slices have functional α7 nAChRs. In the current study, functional α7 nAChRs on astrocytes in the CA1 region of the rat hippocampus were studied in acute slices using whole-cell patch-clamp recording and two-photon calcium imaging techniques. We found that astrocytes and NG2 cells expressed functional α7 nAChRs; however, the amplitude of the responses was small. The amplitude of the α7 responses was enhanced by the α7-selective positive allosteric modulator (PAM) PNU-120596. Under these conditions, we found that in comparing the properties of the α7 nAChR-mediated responses between astrocytes, NG2, and interneurons, there were differences in the kinetics and increases in intracellular calcium levels. This is the first demonstration of functional α7 nAChR-mediated current responses in astrocytes in acute hippocampal slices, along with a comparison of the properties and regulation of these responses between hippocampal astrocytes, interneurons, and NG2 cells. These data may shed light on the role of α7 nAChRs in AD and neuroprotection.

Methods

Slice Preparation

All experiments were carried out in accordance with guidelines approved by the NIEHS Animal Care and Use Committee, which includes minimizing the number of animals used and their suffering. Standard techniques were used to prepare 310 μm thick acute hippocampal slices from 14–21-day-old rats (Shen et al. 2009). Briefly, rats were anesthetized with halothane (Sigma) and decapitated. Brains were quickly removed and placed into an ice-cold oxygenated artificial cerebral spinal fluid (ACSF) containing (in mM): 126 NaCl, 3.5 KCl, 1.3 $MgCl_2$, 2 $CaCl_2$, 1.2 NaH_2PO_4, 25 $NaHCO_3$, and 11 glucose. Slices were placed onto nylon mesh immersed in oxygenated ACSF at room temperature

(23–25°C) and then used for recordings after at least 1 h of recovery period and within about 6 h.

Electrophysiology

Whole-cell patch-clamp recordings were performed on hippocampal CA1 stratum radiatum layer astrocytes, interneurons, or NG2-expressing (i.e., NG2) cells in acute slices. Patch pipettes (Garner 8250 glass, with resistances of 3–7 MΩ for interneurons, and 6–10 MΩ for astrocytes and NG2 cells) were filled with an intracellular solution (ICS) that contained (in mM): 120 potassium gluconate, 2 NaCl, 2 MgATP, 0.3 Na_2GTP, 1 EGTA and 10 HEPES; pH was adjusted to 7.2–7.3 with KOH (1 M), and osmolarity was adjusted to ~285 mOsm with KCl (2 M). Slices were superfused at room temperature with oxygenated ACSF. Using an Eclipse E600FN upright microscope (Nikon, Japan) with a×40 fluorescent water-immersion objective and an iXon cooled 14-bit digital camera (Andor Technology, UK), real-time infrared differential interference contrast (IR-DIC) images were acquired with iQ imaging software (Andor). Cells were clamped using an Axopatch 200B amplifier (Axon Instruments, Union City, CA) at a holding potential of –70 mV (corrected for a 10 mV junction potential) for interneurons and –90 mV for astrocytes and NG2 cells using pClamp 10 software (Axon Instruments). Action potentials were recorded under current-clamp conditions, and current was injected to depolarize neurons to induce spiking; neurons were defined as regular-spiking if the rate of action potential firing evoked by minimal depolarization was <40 Hz (Khiroug et al. 2003). After identifying the firing pattern, TTX (1 μM) was added to the ACSF to block action potential firing.

The α7 nAChR-mediated responses were induced by a brief pressure application (50 ms at 5–20 psi pressure) of choline (10 mM), which was delivered via a glass pipette placed 5–10 μm from the cell body using a Picospritzer II (General Valve Co., Fairfield NJ, USA). The interval between choline applications was 80 s, unless when in the presence of PNU-120596, the interval was 5 min. The pressure application of control ACSF was given to every cell, and it never produced any electrical responses. Bath-applied drugs were diluted at final concentrations in ACSF and were delivered to the cell through a gravity-fed perfusion system. Drugs applied intracellularly were diluted at final concentrations in ICS and dialyzed through the tip of the patch pipette for ~20 min after obtaining the whole-cell recording configuration. For interneurons, cells were discarded if the initial responses were below 200 pA, while for astrocytes and NG2 cells, cells were discarded if the responses were below 50 pA 30 min after PNU-120596 application.

Two-photon and Calcium Imaging

To visualize the soma and processes of the selected cells for patch-clamp recordings, Alexa Fluor-594 (100 μM) was dialyzed into the cell via the patch pipette. Two-photon imaging was done 20 min after obtaining the whole-cell recording configuration using a Zeiss LSM 510 NLO META system. To visualize intact astrocytes specifically, slices were incubated with sulforhodamine 101 (SR101, 3 μM for 30 min; Invitrogen) at 34–37°C; SR101 previously has been found to label only astrocytes and not interneurons nor NG2 cells in the hippocampus (Kafitz et al. 2008; Henneberger et al. 2010). For imaging changes in intracellular calcium levels, fluo-4 AM (Invitrogen, 11 μM), the membrane permeable form of fluo-4, was locally applied with pressure (for 5–10 s using a Picospritzer II) to the outside of the cells. The two-photon system was coupled to an Axioskop 2FS microscope (Carl Zeiss, Inc., Thornwood, NY) using a Ti:sapphire Chameleon two-photon laser system (Coherent, Inc., Auburn, CA). The laser wavelength for two-photon imaging was tuned to 800 nm. The fluorescence from the indicators was separated by a dichroic mirror at 560 nm (NFT 560), filtered by bandpass filters of BP 500–550 IR (wavelength range=500–550 nm)

for green (fluo-4), and BP 570-640 IR (wavelength range=570–640 nm) for red (Alexa Fluor-594 or SR101), and detected with separated photomultipliers.

Data Analysis

Patch-clamp data were analyzed using Clampfit 10.0 (Axon Instruments, Union City, CA), and imaging data were processed using ImageJ 1.44a (Wayne Rasband; National Institutes of Health, USA; http://rsb.info.nih.gov/ij; Java 1.6.0_05 (32-bit) (1997–2010)). Averaged data are presented as mean ± s.e.m., and the statistical difference between the population averages was estimated with the *t* test (for paired or independent samples) or ANOVA when appropriate. Two-tailed tests were routinely used, and sample pairing was used where appropriate (*p* values of <0.05 were considered significant).

Results

Identification of Astrocytes and NG2 Cells in Rat CA1 Hippocampal CA1 Slices

The identification of astrocytes, NG2-expressing (i.e., NG2) cells, and interneurons in acute slices was done using a variety of electrophysiological (i.e., using whole-cell patch-clamp recordings) and morphological (i.e., using two-photon imaging) criteria from the stratum radiatum layer of the rat CA1 hippocampus. As we have previously described (Sudweeks et al. 2002; Khiroug et al. 2003), the depolarization of interneurons under current-clamp conditions will induce action potential firing; all of the interneurones analyzed for firing properties (10 cells) had a regular-spiking action potential firing profile (the average firing rate was 28±4 Hz; Fig. 1a). However, in astrocytes, which were initially chosen because of their smaller somal diameter of 10 μM, depolarization did not evoke any spiking; all our recorded results had passive ohmic properties (Fig. 1b). Under voltage-clamp, while depolarization did not elicit any transient outward currents in astrocytes (Fig. 1c), transient A-type currents were found in some smaller cells which appeared morphologically similar to astrocytes, suggesting that they were NG2 cells (Fig. 1d) (Vélez-Fort et al. 2009). As expected (Kang et al. 1998), astrocytes had a significantly larger negative resting membrane potential than interneurons, whereas NG2 cells were in between (Fig. 1e). In addition, the input resistance of NG2 cells (442±80 MΩ; 10 cells) was as expected (Lin and Bergles 2004) much larger than for astrocytes (24.8±11 MΩ; 18 cells).

A variety of morphological criteria were also used to identify astrocytes and NG2 cells. Cells were filled with Alexa Fluor 594 via the patch pipette during whole-cell recordings and were imaged using IR-DIC and two-photon microscopic imaging (Fig. 2). The shape of the interneuron soma (Fig. 2a) was clearly distinct from that of either astrocytes (Fig. 2b) or NG2 cells (Fig. 2c); the diameter of the interneuronal soma was larger (20 μm) than either astrocytes or NG2 cells (both 10 μm), with several long and clear processes. Furthermore, NG2 cells appeared to have fewer processes than astrocytes. Astrocytes could selectively be labeled with sulforhodamine 101 (SR101, 3 μM; see methods), which does not label NG2 cells nor interneurons in the hippocampus (Fig. 2d; Kafitz et al. 2008; Henneberger et al. 2010).

Functional α7 nAChR-mediated Responses on Astrocytes and NG2 Cells in Rat Hippocampal CA1 Slices

The α7 subtype of the nicotinic ACh receptors were selectively activated under whole-cell patch-clamp recording conditions as was done previously using choline (Shen et al. 2009). The pressure application of choline (10 mM for 50 ms; see Methods) elicited rapidly activating and decaying inward currents in interneurons (Fig. 3a); however, choline only activated very small responses in either astrocytes (Fig. 3b) or NG2 cells (Fig. 3c). The average response amplitude was 308±30 pA (six cells) in interneurons, 16.0± 2.0 pA (14

cells) in astrocytes, and 9.83±2.4 pA (six cells) in NG2 cells. The small size of choline-induced responses in astrocytes and NG2 cells were difficult to study. If they were due to activation of α7 nAChRs, the amplitude of the responses should be enhanced by the α7-selective PAM PNU-120596. At a concentration of 2 μM, PNU-120596 significantly enhanced the amplitude of choline responses in interneurons to 846±79 pA (six cells), in astrocytes to 343± 61 pA (14 cells), and in NG2 cells to 126±67 pA (six cells) (Fig. 3g–i). The potentiation induced by PNU-120596 usually began to take effect after 5 min, and usually peaked after 30–60 min. Furthermore, PNU-120596-enhanced choline responses were completely blocked by the α7-selective antagonist methyllycaconitine (10 nM) in both astrocytes and NG2 cells (five cells). Therefore, these data indicate that both astrocytes and NG2 cells express functional α7 nAChRs, although at a much lower density than interneurons in the rat CA1 hippocampus.

While the brief (50 or 500 ms) pressure application of choline activated α7 responses that rapidly activated with a rise-time (10–90%) in interneurons of 14 ms (Shen et al. 2009), the responses activated much more slowly, with a rise-time of 430±100 ms (eight cells; Fig. 3d) after potentiation with PNU-120596. However, the PNU-120596-enhanced choline responses in astrocytes activated even much more slowly, with a rise-time of 4,850±470 ms (seven cells; Fig. 3e). Interestingly, the rise-time in NG2 cells (591±120 ms; four cells) was similar to interneurons and significantly faster than in astrocytes (Fig. 3f). While the half-time of decay of responses was similar in interneurons (12.6±1.8 s) and astrocytes (17.0±1.8 s), the half-time of decay was significantly faster in NG2 cells (1.22±0.28 s). Therefore, the kinetics of the PNU-120596-enhanced α7 responses was significantly different among the different cell populations studied here.

Activation of the α7 nAChR Increases Intracellular Calcium Levels in Astrocytes

Astrocytes, which were labeled with SR101, were loaded with the calcium indicator fluo-4 AM (Invitrogen, 11 μM), the membrane permeable form of fluo-4, by local pressure application (for 5–10 s using a Picospritzer II) to the outside of the cells. When the PNU-120596-enhanced α7 nAChR-mediated responses were activated, there was a significant increase in the intracellular calcium levels by 39±3% (three cells; Fig. 4a) from baseline. When the α7 nAChRs were activated in fluo-4-loaded interneurons, as expected due to their larger response amplitude, the increase in intracellular calcium levels was 263±24% (three cells; Fig. 4b), a response which was significantly larger than in astrocytes. Therefore, the activation of the PNU-120596-enhanced α7 nAChRs significantly increased intracellular calcium levels both in astrocytes and interneurons (Fig. 4c).

Discussion

We have shown for the first time in hippocampal slices that astrocytes in the CA1 region express functional α7-containing nAChRs. Although cultured astrocytes and microglia (Sharma and Vijayaraghavan 2001; Shytle et al. 2004) have been shown to express functional nAChRs, and a recent report (Vélez-Fort et al. 2009) found that chondroitin sulfate proteoglycan NG2-expressing (i.e., NG2) cells in slices expressed functional α7 nAChRs, previous work has failed to detect nAChR-mediated responses in astrocytes in acute slices (Araque et al. 2002). Furthermore, in a preliminary report (Parri et al. 2011), the activation of α7 nAChRs illicted increases in intracellular calcium levels in astrocytes in hippocampal slice preparations. Here, we compared the properties of the α7 nAChRs in CA1 hippocampal astrocytes, interneurons, and NG2 cells. The amplitude of the current responses in both astrocytes and NG2 cells were small and required augmentation with PNU-120596, the α7-selective PAM. For the PNU-120596-enhanced α7 responses, the kinetics of responses were variable since the activation was significantly slower in astrocytes (versus interneurons or NG2 cells), while the decay of responses was significantly

faster in NG2 cells. Furthermore, activation of the α7 nAChR increases intracellular calcium levels in astrocytes, although as expected from the low density of functional receptors, the increased calcium levels were significantly less than in interneurons.

The primary cholinergic input to the hippocampus arises from the medial septum and diagonal band of Broca (Frotscher and Léránth 1985). Stimulation of these septal cholinergic inputs to hippocampal slices activated muscarinic acetylcholine receptors (mAChRs) on astrocytes in the CA1 stratum oriens layer, indicating that endogenous synaptically released ACh is able to activate cholinergic receptors on these astrocytes (Araque et al. 2002). While this release of ACh did not appear to activate functional nAChRs on these astrocytes, it is possible that the lack of observable nAChR-mediated currents could have been due to the low expression of functional receptors as we observed here in astrocytes in the CA1 stratum radiatum. While recording from hippocampal CA1 stratum radiatum inter-neurons, the stimulation of cholinergic fibers activated α7 nAChR-mediated synaptic potentials (Frazier et al. 1998), indicating that cholinergic inputs which can release ACh synaptically innervate the stratum radiatum. Therefore, this suggests that the α7 nAChRs functionally expressed by the astrocytes that we have reported here could be activated by synaptically released ACh, as well as by exogenous nAChR ligands. While the extent of the depolarization would likely be minimal based on the low expression of the nAChRs themselves, the increase in cytoplasmic calcium levels might be more significant physiologically.

Increases in calcium levels in astrocytes (in part through activation of mAChRs) can regulate synaptic transmission and plasticity, in particular at synapses in the CA1 hippocampal pyramidal cell layer (Shelton and McCarthy 2000; Araque et al. 2002, Perea and Araque 2005; Agulhon et al. 2008). Therefore, the activation of the α7 nAChR might be increasing calcium levels to an extent that has a significant impact on synaptic transmission in the CA1 region. The nAChRs have been reported to regulate multiple forms of synaptic plasticity (Fujii and Sumikawa 2001; Ji et al. 2001; McGehee 2002; Cobb and Davies 2005; Gu and Yakel 2011). In the hippocampal CA1 region, activating the septal cholinergic input induced different types of α7 nAChR-dependent synaptic plasticity, depending on the timing of cholinergic input (Gu and Yakel 2011). Furthermore, in the hippocampus, α7 nAChRs on presynaptic terminals can increase the probability of producing LTP, and can block short- and long-term potentiation in the pyramidal cells (Ji et al. 2001). The hippocampal α7 nAChRs are also known to have a critical role in working and reference memory (Levin 2002, Levin et al. 2009). Since the cognitive deficits associated with AD may be related to dysfunction of the α7 nAChRs (Jonnala and Buccafusco 2001; Kihara et al. 2001; Dineley 2007; Parri et al. 2011), perhaps it is the receptors functionally expressed on astrocytes that are in part responsible for regulating cognitive function.

The α7 nAChRs are also thought to be participating in various mechanisms of neuroprotection (Dineley 2007; Shen et al. 2009; Parri et al. 2011). The nicotine-mediated neuroprotection against glutamate excitotoxicity is calcium dependent (and appears to involve the phosphatase calcineurin) and is thought to be acting through the α7 nAChRs (Dajas-Bailador et al. 2000; Stevens et al. 2003). Furthermore, the protective effect of nicotine or 17β-estradiol against Aβ has been found to involve the α7 nAChR (Kihara et al. 1997; Svensson and Nordberg 1999; Jonnala and Buccafusco 2001). In addition, the excessive stimulation of α7 nAChRs can lead to calcium overload (due to their high calcium permeability) and excitotoxicity (Lukas et al. 2001; Fucile et al. 2006; Ng et al. 2007). Interestingly, there may also be a role for the α7 nAChRs in inflammation in the brain as in the periphery (Shen et al. 2009). In the periphery, ACh via activation of the α7 nAChRs inhibits cytokine synthesis (Wang et al. 2003), while in the brain (and in particular the hippocampus), nicotine or ACh via activation of the α7 nAChRs blocked the release of

proinflammatorycytokines (Shytle et al. 2004; Tyagi et al. 2010). Whether these various actions of the α7 nAChRs (i.e., neuroprotection, excitotoxicity, and inflammation) are through their expression on neuronal or non-neuronal cells is presently unknown; however, the expression on astrocytes will likely be playing a major role.

Thusfar,the onlyreportindicatingthatnon-neuronalcellsin acute hippocampal slices express functional nAChRs was in NG2 cells (Vélez-Fort et al. 2009); previously functional expression had only been observed for cultured astrocytes and microglia (Sharma and Vijayaraghavan 2001; Shytle et al. 2004). In cultured astrocytes, α7 nAChR-mediated current responses averaged 490 pA (Sharma and Vijayaraghavan 2001), much larger than that reported here for astrocytes in acute slices (16 pA; prior to PNU-120596 enhancement). Therefore, it appears as if culture conditions are altering the expression level of the α7 nAChRs, indicating the importance of studying the receptors in situ for understanding their physiological relevance.

In conclusion, we have demonstrated that in acute hippocampal slices, astrocytes expressed functional α7 nAChRs, and that the activation of these responses increased intracellular calcium levels. These data may shed light on the role of α7 nAChRs in neuroprotection.

Acknowledgments

References

Agulhon C, Petravicz J, McMullen AB, Sweger EJ, Minton SK, Taves SR, Casper KB, Fiacco TA, McCarthy KD. What is the role of astrocyte calcium in neurophysiology? Neuron. 2008; 59:932–946. [PubMed: 18817732]

Araque A, Martín ED, Perea G, Arellano JI, Buño W. Synaptically released acetylcholine evokes Ca2+ elevations in astrocytes in hippocampal slices. J Neurosci. 2002; 22:2443–2450. [PubMed: 11923408]

Cobb SR, Davies CH. Cholinergic modulation of hippocampal cells and circuits. J Physiol (Lond). 2005; 562:81–88. [PubMed: 15528238]

Dajas-Bailador FA, Lima PA, Wonnacott S. The α7 nicotinic acetylcholine receptor subtype mediates nicotine protection against NMDA excitotoxicity in primary hippocampal cultures through a Ca^{2+}-dependent mechanism. Neuropharmacol. 2000; 39:2799–2807.

Dani JA, Bertrand D. Nicotinic acetylcholine receptors and nicotinic cholinergic mechanisms of the central nervous system. Annu Rev Pharmacol Toxicol. 2007; 47:699–729. [PubMed: 17009926]

Dineley KT. Beta-amyloid peptide—nicotinic acetylcholine receptor interaction: the two faces of health and disease. Front Biosci. 2007; 12:5030–5038. [PubMed: 17569627]

Dziewczapolski G, Glogowski CM, Masliah E, Heinemann SF. Deletion of the α7 nicotinic acetylcholine receptor gene improves cognitive deficits and synaptic pathology in a mouse model of Alzheimer's disease. J Neurosci. 2009; 29:8805–8815. [PubMed: 19587288]

Fiacco TA, Agulhon C, McCarthy KD. Sorting out astrocyte physiology from pharmacology. Annu Rev Pharmacol Toxicol. 2009; 49:151–74. [PubMed: 18834310]

Frazier CJ, Rollins YD, Breese CR, Leonard S, Freedman R, Dunwiddie TV. Acetylcholine activates an α-bungarotoxin-sensitive nicotinic current in rat hippocampal interneurons, but not pyramidal cells. J Neurosci. 1998; 18:1187–1195. [PubMed: 9454829]

Frotscher M, Léránth C. Cholinergic innervation of the rat hippocampus as revealed by choline acetyltransferase immunocytochemistry: a combined light and electron microscopic study. J Comp Neurol. 1985; 239:237–246. [PubMed: 4044938]

Fucile S, Sucapane A, Grassi F, Eusebi F, Engel AG. The human adult subtype ACh receptor channel has high Ca^{2+} permeability and predisposes to endplate Ca^{2+} overloading. J Physiol (Lond). 2006; 573:35–43. [PubMed: 16527851]

Fujii S, Sumikawa K. Nicotine accelerates reversal of long-term potentiation and enhances long-term depression in the rat hippo-campal CA1 region. Brain Res. 2001; 894:340–346. [PubMed: 11251213]

Gay EA, Yakel JL. Gating of nicotinic ACh receptors; new insights into structural transitions triggered by agonist binding that induce channel opening. J Physiology (Topical Review). 2007; 584:727–733.

Giniatullin R, Nistri A, Yakel JL. Desensitization of nicotinic ACh receptors: shaping cholinergic signaling. Trends Neurosci. 2005; 28:371–378. [PubMed: 15979501]

Gu Z, Yakel JL. Timing-dependent septal cholinergic induction of dynamic hippocampal synaptic plasticity. Neuron. 2011; 71:155–165. [PubMed: 21745645]

Henneberger C, Papouin T, Oliet SH, Rusakov DA. Long-term potentiation depends on release of D-serine from astrocytes. Nature. 2010; 463:232–236. [PubMed: 20075918]

Hernandez CM, Kayed R, Zheng H, Sweatt JD, Dineley KT. Loss of α7 nicotinic receptors enhances beta-amyloid oligomer accumulation, exacerbating early-stage cognitive decline and septo-hippocampal pathology in a mouse model of Alzheimer's disease. J Neurosci. 2010; 30:2442–2453. [PubMed: 20164328]

Ji D, Lape R, Dani JA. Timing and location of nicotinic activity enhances or depresses hippocampal synaptic plasticity. Neuron. 2001; 31:131–141. [PubMed: 11498056]

Jones S, Sudweeks S, Yakel JL. Nicotinic receptors in the brain: correlating physiology with function. Trends Neurosci. 1999; 22:555–561. [PubMed: 10542436]

Jonnala RR, Buccafusco JJ. Relationship between the increased cell surface α7 nicotinic receptor expression and neuroprotection induced by several nicotinic receptor agonists. J Neurosci Res. 2001; 66:565–572. [PubMed: 11746376]

Kafitz KW, Meier SD, Stephan J, Rose CR. Developmental profile and properties of sulforhodamine 101—labeled glial cells in acute brain slices of rat hippocampus. J Neurosci Methods. 2008; 169:84–92. [PubMed: 18187203]

Kang J, Jiang L, Goldman SA, Nedergaard M. Astrocyte-mediated potentiation of inhibitory synaptic transmission. Nat Neurosci. 1998; 1:683–92. [PubMed: 10196584]

Kihara T, Shimohama S, Sawada H, Kimura J, Kume T, Kochiyama H, Maeda T, Akaike A. Nicotinic receptor stimulation protects neurons against beta-amyloid toxicity. Ann Neurol. 1997; 42:159–163. [PubMed: 9266724]

Kihara T, Shimohama S, Sawada H, Honda K, Nakamizo T, Shibasaki H, Kume T, Akaike A. Alpha 7 nicotinic receptor transduces signals to phosphatidylinositol 3-kinase to block A beta-amyloid-induced neurotoxicity. J Biol Chem. 2001; 276:13541–13546. [PubMed: 11278378]

Khiroug L, Giniatullin R, Klein RC, Fayuk D, Yakel JL. Functional mapping and Ca^{2+} regulation of nicotinic acetylcholine receptor channels in rat hippocampal CA1 neurons. J Neurosci. 2003; 23:9024–9031. [PubMed: 14534236]

Levin ED. Nicotinic receptor subtypes and cognitive function. J Neurobiol. 2002; 53:633–640. [PubMed: 12436426]

Levin ED, McClernon FJ, Rezvani AH. Nicotinic effects on cognitive function: behavioral characterization, pharmacological specification, and anatomic localization. Psychopharmacology (Berl). 2006; 184:523–539. [PubMed: 16220335]

Levin ED, Petro A, Rezvani AH, Pollard N, Christopher NC, Strauss M, Avery J, Nicholson J, Rose JE. Nicotinic α7- or β2-containing receptor knockout: effects on radial-arm maze learning and long-term nicotine consumption in mice. Behav Brain Res. 2009; 196:207–213. [PubMed: 18831991]

Lin SC, Bergles DE. Synaptic signaling between neurons and glia. Glia. 2004; 47:290–298. [PubMed: 15252819]

Lukas RJ, Lucero L, Buisson B, Galzi JL, Puchacz E, Fryer JD, Changeux JP, Bertrand D. Neurotoxicity of channel mutations in heterologously expressed α7-nicotinic acetylcholine receptors. Eur J Neurosci. 2001; 13:1849–1860. [PubMed: 11403678]

McGehee DS. Nicotinic receptors and hippocampal synaptic plasticity ... it's all in the timing. Trends Neurosci. 2002; 25:171–172. [PubMed: 11998680]

Nagele RG, D'Andrea MR, Lee H, Venkataraman V, Wang HY. Astrocytes accumulate Aβ42 and give rise to astrocytic amyloid plaques in Alzheimer disease brains. Brain Res. 2003; 971:197–209. [PubMed: 12706236]

Nagele RG, Wegiel J, Venkataraman V, Imaki H, Wang KC, Wegiel J. Contribution of glial cells to the development of amyloid plaques in Alzheimer's disease. Neurobiol Aging. 2004; 25:663–674. [PubMed: 15172746]

Ng HJ, Whittemore ER, Tran MB, Hogenkamp DJ, Broide RS, Johnstone TB, Zheng L, Stevens KE, Gee KW. Nootropic α7 nicotinic receptor allosteric modulator derived from GABAA receptor modulators. Proc Natl Acad Sci USA. 2007; 104:8059–8064. [PubMed: 17470817]

Parri HR, Hernandez CM, Kineley KT. Research update: alpha7 nicotinic acetylcholine receptor mechanisms in Alzheimer's disease. Biochem Pharmacol. 2011; 82:931–942. [PubMed: 21763291]

Perea G, Araque A. Properties of synaptically evoked astrocyte calcium signal reveal synaptic information processing by astrocytes. J Neurosci. 2005; 25:2192–2203. [PubMed: 15745945]

Sharma G, Vijayaraghavan S. Nicotinic cholinergic signaling in hippocampal astrocytes involves calcium-induced calcium release from intracellular stores. Proc Natl Acad Sci USA. 2001; 98:4148–4153. [PubMed: 11259680]

Shelton MK, McCarthy KD. Hippocampal astrocytes exhibit Ca^{2+}-elevating muscarinic cholinergic and histaminergic receptors in situ. J Neurochem. 2000; 74:555–563. [PubMed: 10646506]

Shen JX, Tu B, Yakel JL. Inhibition of α7-containing nicotinic ACh receptors by muscarinic M_1 ACh receptors in rat hippocampal CA1 interneurones in slices. J Physiol. 2009; 587:1033–1042. [PubMed: 19124535]

Shytle RD, Mori T, Townsend K, Vendrame M, Sun N, Zeng J, Ehrhart J, Silver AA, Sanberg PR, Tan J. Cholinergic modulation of microglial activation by alpha 7 nicotinic receptors. J Neurochem. 2004; 89:337–343. [PubMed: 15056277]

Stevens TR, Krueger SR, Fitzsimonds RM, Picciotto MR. Neuroprotection by nicotine in mouse primary cortical cultures involves activation of calcineurin and L-type calcium channel inactivation. J Neurosci. 2003; 23:10093–10099. [PubMed: 14602824]

Sudweeks SN, Hooft JA, Yakel JL. Serotonin 5-HT_3 receptors in rat CA1 hippocampal interneurons: functional and molecular characterization. J Physiol. 2002; 544:715–726. [PubMed: 12411518]

Svensson AL, Nordberg A. Beta-estradiol attenuate amyloid beta-peptide toxicity via nicotinic receptors. Neuroreport. 1999; 10:3485–3489. [PubMed: 10619630]

Teaktong T, Graham A, Court J, Perry R, Jaros E, Johnson M, Hall R, Perry E. Alzheimer's disease is associated with a selective increase in alpha7 nicotinic acetylcholine receptor immunoreactivity in astrocytes. Glia. 2003; 41:207–211. [PubMed: 12509811]

Tyagi E, Agrawal R, Nath C, Shukla R. Inhibitory role of cholinergic system mediated via α7 nicotinic acetylcholine receptor in LPS-induced neuro-inflammation. Innate Immun. 2010; 16:3–13. [PubMed: 19586999]

Vélez-Fort M, Audinat E, Angulo MC. Functional alpha 7-containing nicotinic receptors of NG2-expressing cells in the hippocampus. Glia. 2009; 57:1104–1114. [PubMed: 19170184]

Wang H, Yu M, Ochani M, Amella CA, Tanovic M, Susarla S, Li JH, Wang H, Yang H, Ulloa L, Al-Abed Y, Czura CJ, Tracey KJ. Nicotinic acetylcholine receptor α7 subunit is an essential regulator of inflammation. Nature. 2003; 421:384–388. [PubMed: 12508119]

Xiu J, Nordberg A, Zhang JT, Guan ZZ. Expression of nicotinic receptors on primary cultures of rat astrocytes and upregulation of the α7, α4 and β2 subunits in response to nanomolar concentrations of the β-amyloid peptide$_{1-42}$. Neurochem Int. 2005; 47:281–290. [PubMed: 15955596]

Yakel JL. Gating of nicotinic ACh receptors: latest insights into ligand binding and function. J Physiology (Symposium Review). 2010; 588:597–602.

Yu WF, Guan ZZ, Bogdanovic N, Nordberg A. High selective expression of α7 nicotinic receptors on astrocytes in the brains of patients with sporadic Alzheimer's disease and patients carrying Swedish APP 670/671 mutation: a possible association with neuritic plaques. Exp Neurol. 2005; 192:215–225. [PubMed: 15698636]
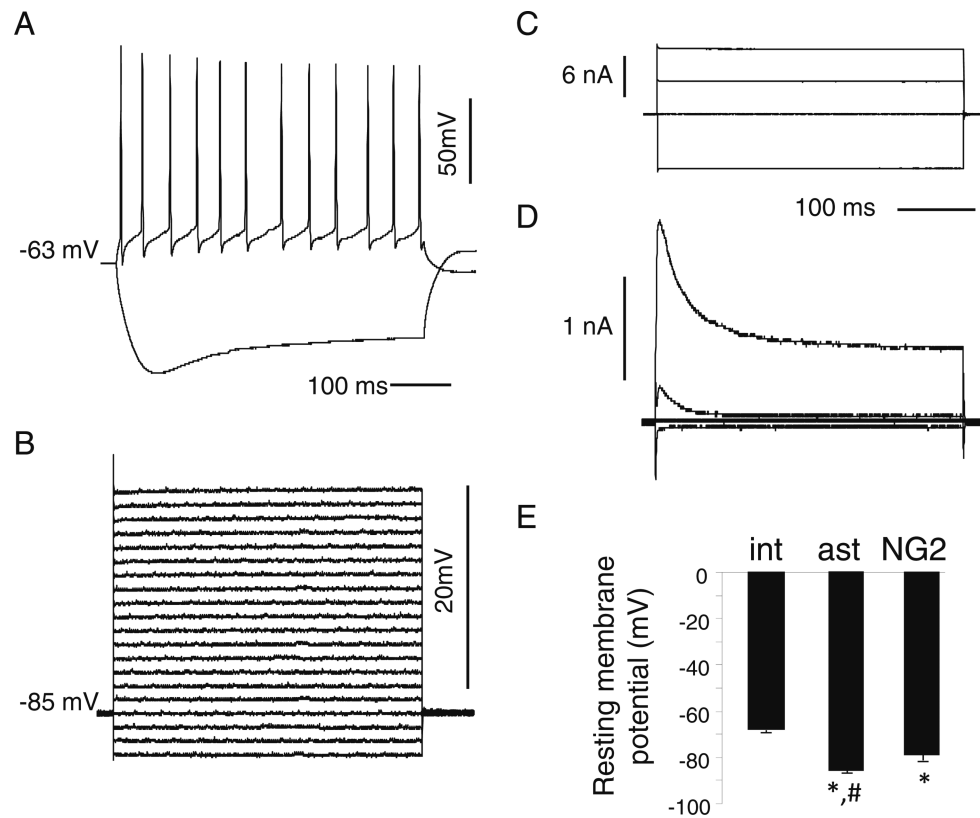
A

-63 mV

50mV

100 ms

B

20mV

-85 mV

C

6 nA

100 ms

D

1 nA

E

int ast NG2

Resting membrane potential (mV)

0

-20

-40

-60

-80

-100

*,#

*

Fig. 1.
Electrophysiological properties of interneurons, astrocytes, and NG2 cells in acute CA1 rat hippocampal slices. **a** Firing pattern of a representative interneuron (current-clamp configuration). Action potentials were evoked by current injection (+100 pA and –150 pA for the upper and lower traces, respectively). B,C. Voltage responses elicited by current steps of ±150 pA under current-clamp (**b**) or current responses elicited by voltage steps under voltage-clamp (**c**) (from –80 mV to either–mV, –20 mV, or +40 mV) in representative astrocytes. **d** Current responses elicited by voltage steps under voltage-clamp (same as in C) in a representative NG2 cell. **e** Average resting membrane potentials of interneurons ("*int*"; 14 cells), astrocytes ("*ast*"; 12 cells), NG2 cells (10 cells). Plot shows mean ± SEM and was subjected to a one-way ANOVA. The *asterisk* indicates significantly different compared to interneurons, $p<0.01$. The *number sign* indicates significantly different compared to NG2 cells, $p<0.01$
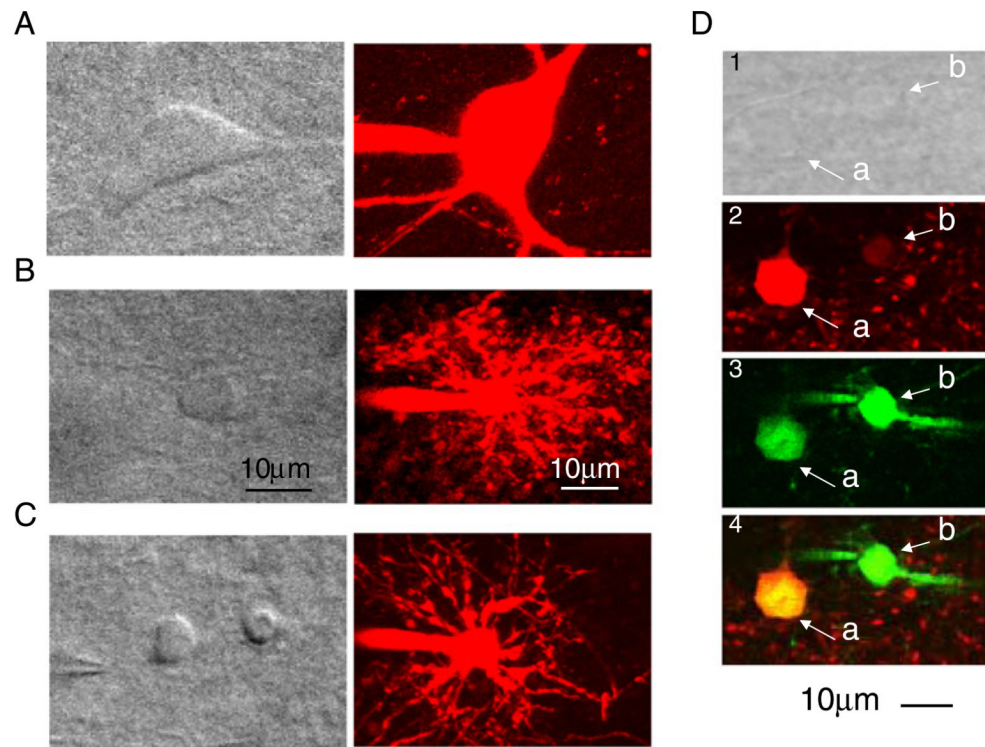
Fig. 2.
Morphological features of astrocytes and NG2 cells in acute hippocampal slices. IR-DIC (*left panels*) and two-photon (*right panels*) images of an interneuron (**a**), astrocytes (**b**), and NG2 cell (**c**). The two-photon images were obtained by loading cells with Alexa Fluor-594 (100 μM) during whole-cell recordings. **d** IR-DIC (*top; panel 1*) and two-photon images of an astrocyte (*a*) and an NG2 cell (*b*). In *panel 2*, the astrocyte (*a, red*) is labeled with SR101; the NG2 cell (*b*) is not labeled with SR101 as expected. In *panel 3*, an astrocyte (*a*) and an NG2 cell (*b*) are labeled with fluo-4 AM (which was locally applied with pressure; see Methods). The identity of all cells was confirmed by whole-cell current-clamp recording. *Panel 4* is the merging of *panels 2 and 3*
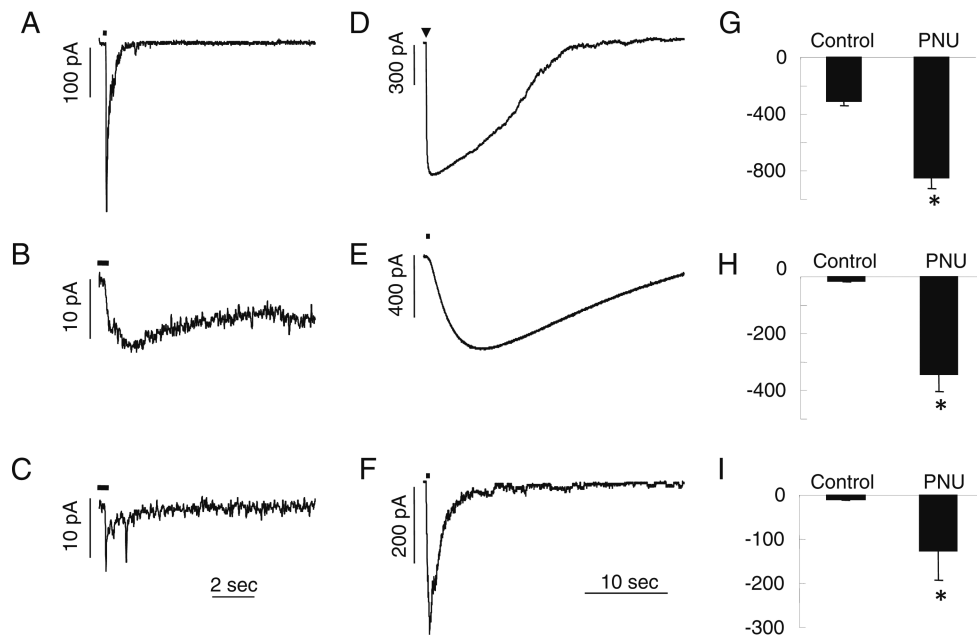
Fig. 3.

Functional α7 nAChR-mediated responses on interneurons, astrocytes, and NG2 cells in slices. **a** Representative rapidly activating and decaying inward current α7 nAChR-mediated responses in an interneuron due to the pressure application of choline (10 mM for 50 ms; indicated by the *bar*). The representative α7 responses in an astrocyte (**b**) and an NG2 cell (**c**) due to pressure-applied choline (10 mM for 500 ms). **d–f** The α7 responses in interneurons (**d**), astrocytes (**e**), and NG2 cells (**f**) were significantly enhanced and prolonged by the bath application of PNU-120596 (2 μM). **g–i** The averaged peak amplitude data before (control) and after bath application of PNU-120596 (>30 min) to all three cell types. The data are from 5 interneurons (**g**), 14 astrocytes (**h**), and 6 NG2 cells (**i**). The *asterisk* indicates significantly different compared to control, $p<0.05$
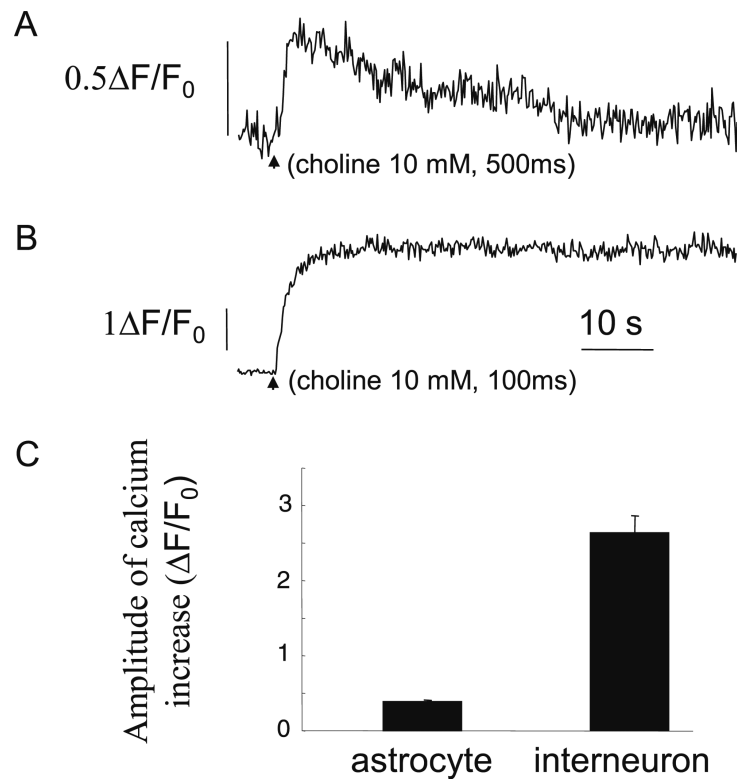
A

$0.5 \Delta F/F_0$

(choline 10 mM, 500ms)

B

$1 \Delta F/F_0$

10 s

(choline 10 mM, 100ms)

C

Amplitude of calcium increase ($\Delta F/F_0$)

astrocyte   interneuron

Fig. 4.
Activation of the α7 nAChRs increases intracellular calcium levels in astrocytes. **a, b** Representative time-courses showing global calcium increases in an astrocyte (**a**) and interneuron (**b**) after choline activation of the PNU-120596-enhanced α7 response (indicated by *arrow*). **c** Bar graph showing averaged relative calcium increases in astrocytes and interneurons